22nd International Symposium on Plasma Chemistry
July 5-10, 2015; Antwerp, Belgium

Antiproliferative effects on multi-cellular tumor spheroids induced by low-temperature plasma

F. Judée[1,2], N. Merbahi[1,2], J-M Plewa[1,2], M. Yousfi[1,2], C. Frongia[3,4], O. Eichwald[1,2], B. Ducommun[3,4,5] and V. Lobjois[3,4]

[1] *Université de Toulouse; LAPLACE-UMR5213, F-31062 Toulouse, France*
[2] *CNRS; LAPLACE-UMR5213, F-31062 Toulouse, France*
[3] *Université de Toulouse; ITAV-USR3505, F-31106 Toulouse, France*
[4] *CNRS; ITAV-USR3505, F-31106 Toulouse, France*
[5] *CHU de Toulouse; F-31059 Toulouse, France*

Abstract: In the present work the antiproliferative effects of low-temperature plasmas on a multicellular tumor spheroid (MCTS) was investigated. A growth inhibition is associated with the loss of Ki67, and the regionalized accumulation of DNA damage detected by histone H2AX phosphorylation. The use of ROS scavenger demonstrate that the ROS generated in the media after play a major role in these observed effects.

Keywords: multi-cellular tumor spheroid, antiproliferative effect, reactive oxygen species

1. Introduction

In the field of biomedical applications, low-temperature plasmas ejected in open air are an interesting source of active species (charged particles, radicals, long-lived excited species, UV photons, electric field, etc) that can easily be launched, for example, on any prokaryote or eukaryote cells, living tissues, biomaterial surfaces, etc. The reader can find exhaustive lists of references on these biomedical applications (for example, in [1-2]) and also on plasma-induced anti-tumor effects that are evocated, hereafter, in the light of a few examples of the literature.
Indeed nowadays, there is a growing interest on research works devoted to the effect of low-temperature plasmas at atmospheric pressure on cancer cells, both in vitro and in vivo.

However, despite the great interest of these works, none provide precise information on the penetration depth, or the species generated by the plasma into the tumor tissue medium, or on the analysis of the effects on cells located, not only on the surface layer of a cancer cell culture, but also inside the tumor tissue volume. Multicellular tumor spheroid (MCTS) is a 3D culture model that accurately reproduces the organization and the heterogeneity of a microtumor domain with cell–cell and cell–microenvironment interactions [3-5]. The use of this model is currently recognized as an important step in the development of anti-cancer strategies between the studies performed on classical monolayer cultured cells and animal models. The present work is aimed at investigating the regionalized antiproliferative effects of low-temperature plasma on the various layers of MCTS.

2. Materials and methods

a. Low-temperature plasma generation

The low-temperature plasma jet is produced by a dielectric barrier discharge configuration already detailed elsewhere [6]. In short, aluminum tape electrodes having a 20 mm width are wrapped on a quartz tube with a 4 mm inner diameter and a 6 mm outer diameter, and separated by a 10 mm space. Helium gas flows through the quartz tube with a flow rate of 3 liter.min−1. High-voltage mono-polar square pulses are applied on the powered electrode with specific voltage magnitude, repetition rate and pulse width (voltage = 8.97 kV, repetition rate = 9.69 kHz, pulse width = 1 µs). A schematic set-up of the plasma jet device is displayed in figure 1(a), while figure 1(b) shows an example of plasma exposure of a spheroid placed inside a well of 96-round bottom well plates.

The gas temperature measured from classical thermo-couple and emission spectroscopy based on the OH(A-X) spectrum is around 30 °C due to the very low power consumption required to generate the plasma jet. Constant distance chosen between the output of the glass tube and the culture medium of spheroids during plasma exposure is fixed at 2 cm, as shown in figure 1(b). At this distance, the dilution of helium plasma in the air leads to a rich population in the gaseous phase of more particularly reactive oxygen species (ROS), such as atomic oxygen, ozone, hydroxyl radical, nitrogen oxide, hydrogen peroxide and several long-lived excited species of molecular and atomic oxygen. They directly interact with the culture medium, immersing the studied spheroid inside each well of the 96-well plates. Such interactions lead, in turn, to the generation of ROS in liquid phase, as, for instance, hydrogen peroxide with hydroxyl, super-oxide and nitrogen oxide radicals.

b. Cell culture and spheroids preparation

HCT116 colorectal cancer cells (ATCC) were cultured in DMEM (Invitrogen) containing 10% FCS with 2 mMl−1 glutamine and penicillin/streptomycin in a humidified atmosphere of 5% CO_2 at 37 °C. Spheroids were prepared by centrifugation method in low attachment multi-well

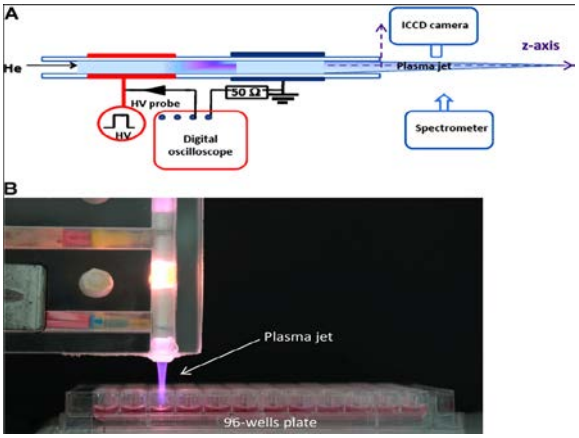

Fig. 1. (a) Schematic set-up for the generation of a low temperature plasma jet (b) Exposure to the low-temperature plasma jet of a spheroid grown in 96-round bottom well plates (distance between the top of the quartz tube and the culture medium of the spheroid = 2 cm).

plates. Briefly, exponentially growing cells were harvested and were distributed in poly-HEMA-coated 96-round bottom well plates (500 cells/well). Plates were centrifuged (600 g for 6 min), and then placed in a humidified atmosphere of 5% CO_2 at 37 °C. Aggregation of the cells occurred within 24 h, and the diameter of the growing spheroids was measured over time with a calibrated eyepiece reticule until they reached the expected size needed to start a given experiment.

c. Immunofluorescence on spheroid cryosections

Spheroids were fixed in formalin (Sigma) for 2 to 3 h, then washed with phosphate buffered saline (PBS) and stored at 4 °C. After fixation, spheroids were incubated in 15% and then 30% sucrose in PBS at 4 °C for 24 h, embedded in Tissue-Tek (Sakura Finetek) and then processed for 5 µm cryosections. After blocking in PSB/1% BSA/0.5% Triton, sections were incubated with antibodies against Ki67 (rabbit polyclonal, Santa Cruz, 1/200 at 4 °C, overnight), cleaved PARP (rabbit monoclonal, Epitomics, 1/1000 at 37 °C, for 1 h), phosphorylatedHistoneH2AX (mouse monoclonal, Millipore, 1/500 overnight at 4 °C). After washes in PBS/0.1% Triton v/v, the secondary antibody was added for 1 h (anti-mouse or anti-rabbit conjugated with Alexa 488, Alexa 594 or Alexa 647, Molecular Probes, 1/800, at room temperature). DNA was stained using 4′,6′-diamidino-2-phénylindole (DAPI). An initial antigen retrieval step (boiling in a solution containing 2 mM citric acid and 8 mM sodium citrate for 3 × 7 mn) was included for the anti-Ki67 antibodies.

d. Image acquisition and analysis

Transmitted light images of spheroids were acquired using a MacroFluo Z16 APO microscope (Leica) fitted with a CoolSNAP ES2 CCD camera (Roper). Fluorescence images of 5 µm spheroid sections were acquired using a DM5000 (Leica) epifluorescence microscope, fitted with a Roper COOLsnap ES CCD camera. Images were processed using the Metavue and ImageJ software packages.

e. Time-lapse experiments

Transmitted light images of spheroids were acquired using an inverted microscope Axiovert (Zeiss) under environmentally-controlled conditions (5% CO2, 37 °C) fitted with a CoolSNAP ES2 CCD camera (Roper) and equipped with a 10X objective.

3. Results

a. Exposure of MCTS to low-temperature plasma

With this experimental setup, spheroids, one per well of a plate, could be exposed to different plasma doses by controlling the exposure time of each well. A masking plate (not shown in figure 1(b)) was always used to avoid cross-exposure between neighboring wells during plasma treatment. It is noteworthy that for the chosen position z = 2 cm between the 96-wells plates and the plasma jet tube output (see figure 1(b)), the estimated power flow (as shown in section 2.2) is about 0.5 mWatt.cm^{-2} in the case of the considered operating parameters of the power supply [6]. Therefore the plasma dose in mJoule.cm−2 (or mJ.cm^{-2}) is determined by multiplying this power density (0.5mW.cm^{-2}) by the exposure time, thus giving, for instance, 30 mJ.cm^{-2} in the case of an exposure time of 60 sec.

b. Low-temperature plasma inhibits MCTS growth

We first evaluated the impact of low-temperature plasma on spheroid growth. To this aim, we subjected HCT116 spheroids to He plasma exposure at duration times varying between 0 to 150 sec, corresponding to plasma doses ranging from 0 to 75 mJ cm^{-2}.

Spheroids measuring 400 µm in diameter were subjected to plasma exposure. At that size, HCT116 spheroids already display a slight proliferation gradient with quiescent cells in the most inner cell layers. Variation of HCT116 spheroid volume was monitored during 8 days following exposure, and shown in figure 2(a). During the time of the analysis of the impact of plasma on spheroids growth, control spheroids continued to grow. As the spheroids size increased, cell heterogeneity inside the spheroids also increased with a more pronounced cell proliferation gradient. The progressive size increase was accompanied by the progressive appearance of cell death in the inner cells of the spheroids at the end of the experiment, as already published elsewhere [7]. This growth dynamic exactly corresponds to previously reported observations (see references [3-5]). Spheroid volume increase was strongly inhibited in a dose-dependent manner. This result was particularly obvious following plasma exposure to a dose above 30 mJ.cm^{-2} that totally inhibited spheroid growth, since a volume reduction was induced on the first day after plasma exposure. The series of micrographs taken at intervals (figure 5(b)) further confirmed these

observations, illustrating partial inhibition at low dose and the total absence of growth of spheroids exposed to low-temperature plasma dose above 30 mJ.cm^{-2}. In addition, with high doses the overall structure of the spheroids appeared modified with a fuzzy outer-most corona and a dense central region.

In order to further characterize the growth inhibitory effect of low-temperature helium plasma, the expression of the proliferation marker Ki67 was analysed by immunofluorescence on spheroid cryosections (figure 3(a)). Ki67 labeling was found to be largely reduced in a dose dependent manner and strongly decreased in the MCTS section examined 16 and 24 h after plasma exposure to 60 mJ cm^{-2}. However, surprisingly, no apoptotic cells were detected using PARP-C staining within spheroids exposed to the same plasma regimen (figure 3(b)), indicating that in our experimental conditions, growth inhibition was clearly associated with cell proliferation inhibition but not with detectable apoptosis.

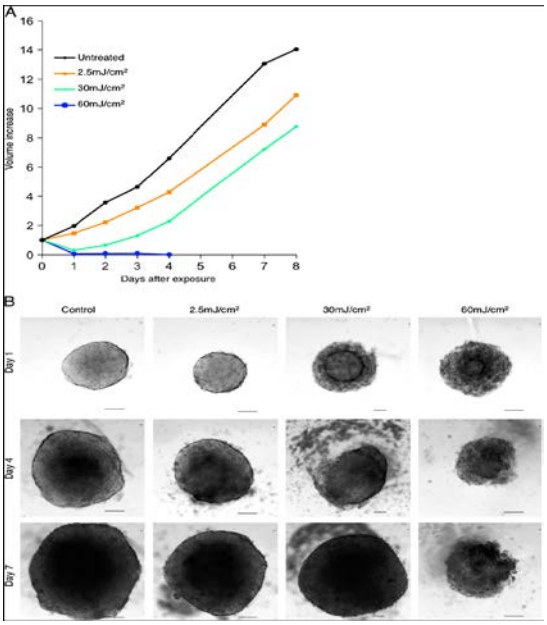

Fig. 2. (a) The time-course of the growth increase in HCT116 spheroids after plasma exposure at the indicated doses. The results correspond to the mean of three to four spheroids per condition. (b) Micrographs illustrating the relative variation in the volume of the HCT116 spheroid one, four and seven days after plasma exposure at the indicated doses. Scale bar, 100 µm.

c. MCTS growth inhibition is associated with regionalized DNA damage

The DNA damaging effect was investigated by immunodetection of the phosphorylated form of histone H2AX on spheroid cryosections. As displayed in figure 3(c), phosphorylated histone H2AX was strongly detected in spheroids 4 h after He plasma exposure. The staining was extremely intense in the outmost cell layers of the Spheroid exposed to the highest plasma dose. Strikingly, this staining was detected at the earliest time-point, but was progressively lost after 16 h and was not detectable after 24 h. On sections from spheroids 16 h after a 60 mJ.cm−2 exposure, the outer-most cells appeared to be less organized at the periphery. In the meantime, spheroid diameter appeared reduced and the fuzzy outmost region previously mentioned (figure 2) was lost. Altogether, these data suggested that the spheroids were peeled off the outmost layers of cells that had DNA damage induced by plasma exposure.

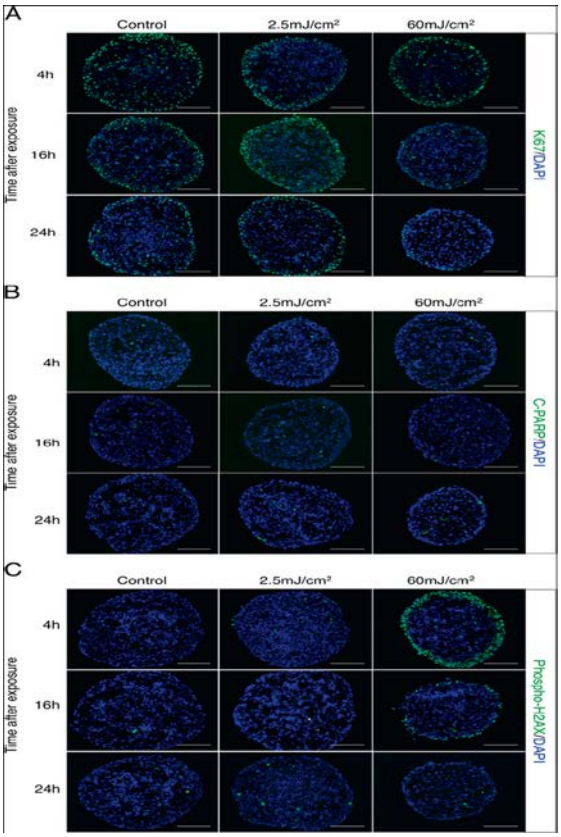

Fig. 3. (a) Visualization of the proliferative cells (Ki67, green), on cryosections from control HCT116 spheroids or spheroids harvested and fixed 4, 16 or 24 h after exposure to helium plasma at the indicated doses. (b) Immunodetection of the apoptotic marker, cleaved-PARP (C-PARP, green), on cryosections after exposure to plasma at the indicated doses. (c) Genotoxic effect analysed by immunodetection of the phosphorylation of the histone variant H2AX (phospho-H2AX, green) on cryosections. The nuclei were stained using DAPI (blue). Representative images from six to eight spheroids from two independent experiments are shown. Scale bar, 100 µm.

d. Growth inhibition and DNA damage are dependent on ROS

In order to investigate the role of ROS in the observed growth inhibitory effect and DNA damage induction, we used the ROS scavenger N-Acetyl Cysteine (NAC) in the

following experiments. We first examined, over time, the growth of HCT116 spheroids exposed to increasing doses of low-temperature helium plasma in the presence of NAC (10 mM). As shown in figure 4(a), in the presence of NAC plasma exposure did not inhibit spheroid growth even at the higher doses. This result was confirmed by the examination of Ki67 staining on spheroids frozen sections (figure 4(b)). As displayed, there was no inhibition of Ki67 staining in the proliferative layers, with the exception of the spheroids exposed to a plasma dose of 60 $mJ.cm^{-2}$ in which a slight lowering of the percentage of Ki67 cells was detectable. Strikingly, the DNA damaging effect of low-temperature helium plasma was also fully reversed by NAC as presented in figure 4(c). In all the tested conditions, no increase in phosphorylated-histone H2AX staining was detected on spheroid sections upon treatment. Altogether, these data further confirm that reactive oxygen species are involved in the growth inhibition and in DNA injury observed in HCT116 MCTS exposed to low-temperature plasma.

4. Discussion

The effects of low-temperature helium plasmas have been evaluated on HCT116 MCTS. We report a strong link between the growth inhibition of MCTS volume and the plasma dose. Indeed, plasma doses ranging from 0 to 75 $mJ.cm^{-2}$ were applied to HCT116 spheroids and resulted in partial growth inhibition for the lowest doses, while the total growth inhibition was from 30 $mJ.cm^{-2}$ plasma exposure. Furthermore, growth inhibition has been correlated with the detection of a regionalized DNA damaging effect detected by immunodetection of the phosphorylated form of histone H2AX. The deleterious consequence of that genotoxic effect was observed by video microscopy, which showed an obvious disorganization of the outermost layers of the MCTS. The latter were gradually disaggregated, leading to a progressive decrease in the MCTS volume. In fact, the spheroid cells of the outermost layers were progressively dying, and released from the spheroid over time. This observation explains why the C-PARP staining presented in figure 3 did not reveal any apoptosis on plasma-exposed MCTS. Furthermore, our results also demonstrate that the DNA damaging effect and the subsequent cell death and growth inhibitory effects are regionalized when helium plasma is applied on a 3D microtumor. Reactive oxygen species have been reported to be involved in the anti-tumoral effect of low-temperature plasma [8-9]. Here from experiments with and without the NAC scavenger, we show that ROS are responsible for the DNA damaging effect observed in the outermost cell layers up to a certain depth inside the MCTS, depending on the applied plasma dose. It is noteworthy that ROS generated by the plasma jet and diffusing in a liquid medium include those usually emphasized in the literature, and also long-lived excited species and atomic oxygen Altogether, our results open various attractive perspectives in the field of low-temperature plasma for antiproliferative purposes.

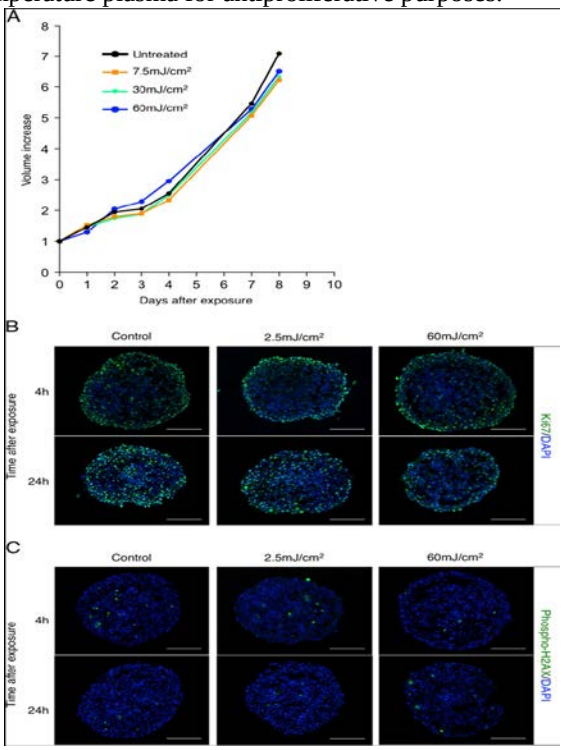

Fig. 4. (a) Time-course of the growth increase of HCT116 spheroids after plasma exposure at indicated doses in the presence of 10mM of NAC in the culture media. The results correspond to the mean of three to four spheroids per condition. (b) Visualisation of the proliferative cells on cryosections in the presence of NAC. (c) Genotoxic effect detected by immunodetection of the phosphorylation of the histone variant H2AX (phospho-H2AX, green) on cryosections in the presence of NAC. Nuclei were stained using DAPI (blue). Scale bar, 100 μm.

5. References

[1] Yousfi M, Merbahi N, Pathak A and Eichwald O *Fundam:. Clin. Pharmacology* **28** 123–5 (2014)

[2] Ishaq M, Evans M M and Ostrikov K K *Int.J. Cancer* **134** 1517–28 (2014)

[3] Desoize B and Jardillier J *Crit. Rev. Oncol. Hematol* **36** 193–207 (2000)

[4] Hirschhaeuser F, Menne H, Dittfeld C, West J, Mueller-Klieser W and Kunz-Schughart L A *J. Biotechnol.* **148** 3–15 (2010)

[5] Drasdo D and Hoehme S *New J. Phys.* **14** 055025 (2012)

[6] Yousfi M, Eichwald O, Merbahi N and Jomaa N *Plasma Sources Sci.Technol*. **21** 045003 (2012)

[7] Lobjois V, Frongia C, Jozan S, Truchet I and Valette *Eur. J. Cancer* 452402–11 (2009)

[8] Graves D B *J. Phys. D: Appl. Phys*. **45** 263001 (2012)

[9] Zhao S et al *PLoS One* **8** e73665 (2013)